

EXPERIMENTAL RESULTS FOR HYBRID SOLAR & GAS WATER HEATING SYSTEMS

Jean-Marc Stephane Lafay

Centro Federal de Educação Tecnológica do Paraná – Via do Conhecimento, km 01 CEP 85501-970 Pato Branco - PR

jean@mecanica.ufrgs.br

Arno Krenzinger

Universidade Federal do Rio Grande do Sul – Sarmiento Leite, 425 CEP 90050-170 Porto Alegre - RS

arno@mecanica.ufrgs.br

César Wilhelm Massen Prieb

Universidade Federal do Rio Grande do Sul – Sarmiento Leite, 425 CEP 90050-170 Porto Alegre - RS

cprieb@ufrgs.br

Abstract. This work aims to collect and analyze experimental data that will serve as a basis for developing a methodology for sizing water heating systems combining solar energy and natural gas. At the experimental phase of this project two water heating systems were assembled. Each system was built with identical 600 liters insulated stainless steel tanks, 2 x 0.9 m² flat-plate solar collectors and 7.5 l/min instant gas heaters. The systems were characterized from the solar collectors efficiency curve, the gas heater efficiency and the tank overall loss coefficient. All of these parameters were experimentally determined within the scope of this project. The solar collectors had the same orientation in both systems, as well as the gauge and length of the copper piping, so it was ensured that the systems only differ in the way the heaters were connected to the tank. The sensors signals were measured by a Hewlett-Packard HP34970A data acquisition unit interfaced to a computer via RS-232. Temperatures, solar irradiance, gas consumption and water consumption data were registered in a forty seconds rate. The obtained experimental results will be used to validate the models employed in the simulation programs, which will be subject of further works.

Keywords. solar energy, solar heating, gas heating, hybrid heating.

1. Introduction

The recent energy crisis Brazil underwent has renovated the interest in alternative energy sources. According to the Brazilian program for electricity conservation PROCEL (2003), about 25 % of the residential electricity consumption is used in electric showers. Solar water heating systems are a good option due to their efficiency and cost-benefit relation. Since the performance of such systems is weather dependant, an auxiliary heat source is required to supply energy to the system at night or cloudy periods. The ordinary auxiliary source is a standard electric heater inside the storage tank. The traditional sizing method of such systems is based on the balance between solar and electric fractions. Modifications to this method are required if other auxiliary energy source (such as LPG or natural gas) is employed due to the different energy costs. The lower cost of the gas when compared to electricity allows the reduction of the solar fraction (and so the collectors area) resulting in lower implementation costs and lower final cost per kJ, as demonstrated by Krenzinger and Lafay (2002).

The solar collector efficiency is a function of the solar irradiance, the ambient temperature and the temperature of the collector inlet water. The lower is the collector inlet temperature the higher is the collector efficiency. Thus the solar contribution to the overall system performance, as a result of the collector performance itself, is also influenced by the gas fraction and the resulting temperature stratification inside the tank. Therefore the performance of the system will depend on the heights of the input and output connections between the gas heater and the tank as well as between the solar collector and the tank.

In order to analyze the behavior of solar-gas hybrid water heating systems, two experimental systems using instant gas heaters as auxiliary energy source were assembled at the Solar Energy Laboratory of the Universidade Federal do Rio Grande do Sul. Both systems are identical except for the way the solar collectors and the gas heater are connected to the storage tank. Temperature sensors were distributed inside the tank and along the water piping. The ambient temperature, the solar irradiation and the gas consumption were also monitored. The sensors signals were collected by a computer controlled data acquisition system.

The obtained data will serve as a reference for the validation of a solar-gas water heating systems simulation computer program. Thus every system component was individually characterized and all of the sensors were carefully calibrated. This software is currently under development at the Solar Energy Laboratory of UFRGS and will be detailed in other work to be presented in this congress.

2. Description of the experimental systems

Each of the solar-gas water heating systems is constituted by two flat-plane collectors connected in *parallel*, an insulated storage tank, an instant gas heater, a pump and a thermostat. The system components are connected together



Figure 1. General view of the *parallel* (left) and *series* (right) systems.

with copper pipes insulated with polyurethane foam tubes. A fiberglass cold water supply tank is shared by both systems. Temperature sensors were installed for monitoring water and ambient air temperatures. The solar irradiance is measured by a photovoltaic pyranometer. All the sensors signals are collected by an automated data acquisition system.

As mentioned before the systems were assembled in two distinct configurations, differing only by the way solar and gas heaters are connected to the tank. In *parallel* configuration the inlet of the solar collector and inlet of the gas heater are connected to the tank bottom and their outlets are connected to the top of the tank. In *series* configuration the inlet of the solar collector is also connected to the tank bottom but its outlet is connected to the tank at half height. The gas heater inlet is connected to the tank at half height while its outlet connects to the top of tank. Figure (1) shows a general view of both systems and in Fig. (2) is represented a diagram of the main hydraulic connections of each system.

2.1 Hot water storage tanks

The employed storage devices are vertical cylindrical stainless steel tanks, insulated with expanded polyurethane (50 mm thick) and wrapped with tin foils. Its dimensions are shown in Fig. (3). The nominal capacity of each tank is 600 liters and the aspect ratio was chosen aiming an enhanced temperature stratification of the water inside the tank. For the analysis of its thermal behavior during the system operation the tank was subdivided in eight equally spaced layers.

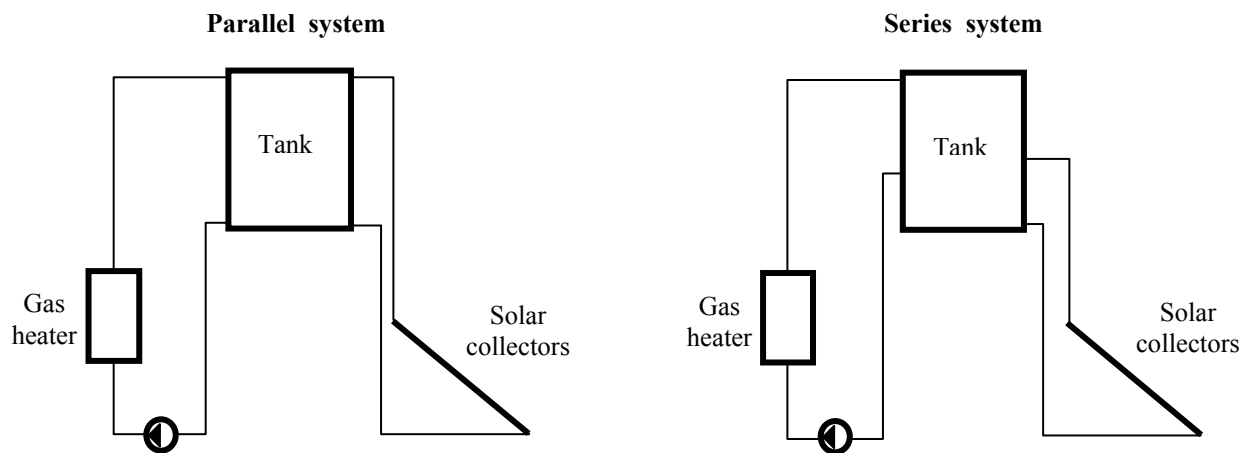


Figure 2. Schematic diagram showing the hydraulic connections of the *parallel* and *series* systems.

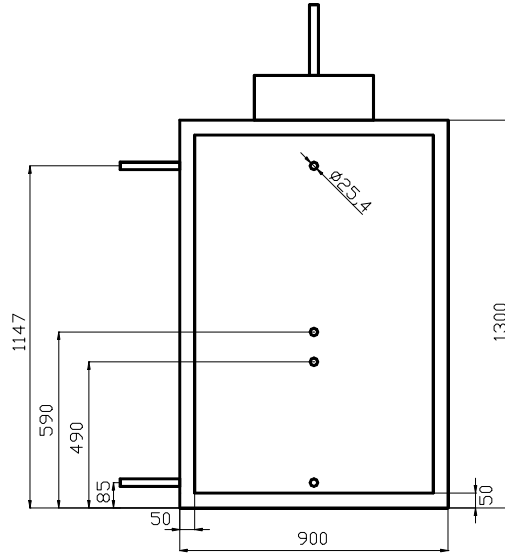


Figure 3. Dimensions of the storage tanks (mm).

2.1.1 Storage tank thermal losses

The overall thermal loss coefficient of one of the tanks used in this work was experimentally evaluated. The employed method consisted in determining the average power required by an electric heater installed inside the tank to maintain the water at a certain temperature. The overall thermal loss coefficient is the result of the division of this power by the difference between room air and water temperatures. Such method has the advantage of being independent of the tank volume and area, as well as the material and thickness of the insulation. The test was performed in a room with a rather constant temperature. The tank was filled with water and a set of three electric heaters, with a total power of about 400 W, was installed immersed in the water at the tank bottom. Placing the heaters at the bottom allowed the convective motion of the water caused by the heating to promote the homogenization of the temperature inside the tank. The heaters were controlled by a thermostat installed at the upper part of the tank, set to 60 °C.

Three platinum resistance sensors placed at equally spaced heights sensed the temperature of the water inside the tank. Another one sensed the room air temperature. A data acquisition system registered the temperatures, as well as the current and voltage applied to the heaters. The data collection started after steady state was established and continued for several days. The energy consumption over the considered period resulted in an average power of 215 W. The average temperatures of the water and the room were 60.4 °C and 24.6 °C respectively, resulting in a loss coefficient of about 6 W/°C.

2.2. Solar collectors

The solar collectors used in this experiment were commercial flat-plate, copper sheet and tubes type collectors. Manufactured by IEM, they are single glazed and insulated at back and sides with glass wool sheets. The external dimensions of the collectors are 0.59 m x 1.5 m.

2.2.1. Collector efficiency

The thermal efficiency of a solar collector is defined as the rate between the useful gain Q_u and the solar radiant energy reaching the collector plane. Thus:

$$\eta = \frac{Q_u}{A_c G_T} = \frac{\dot{m} C_p (T_o - T_i)}{A_c G_T} \quad (1)$$

where \dot{m} is the water flow rate, C_p is the water specific heat, T_o is the outlet temperature and T_i is the inlet temperature. A_c is the collector area and G_T is the radiant flux on the collector plane.

On the other hand, the theory of flat-plane collectors says that the useful heat can be calculated from the difference between the absorbed energy and the thermal losses. According to Duffie and Beckman (1991):

$$Q_u = A_c \left[G_T (\tau\alpha)_e - U_L (T_p - T_a) \right] \quad (2)$$

where $(\tau\alpha)_e$ is the effective transmittance-absorptance product, U_L is the collector overall loss coefficient, T_p is the mean temperature of the absorber plate and T_a is the ambient air temperature.

The value of T_p is difficult to be experimentally determined because of the temperature gradients along the absorber plate. Thus is convenient to define a quantity that relates the actual useful energy gain to the useful gain if the whole absorber surface were at the water inlet temperature T_i instead of the plate mean temperature T_p . This quantity is called the collector heat removal factor, F_R . Therefore the useful gain can be redefined as:

$$Q_u = A_c F_R \left[G_T (\tau\alpha)_e - U_L (T_i - T_a) \right] \quad (3)$$

and the efficiency as:

$$\eta = F_R \left[(\tau\alpha)_e - U_L \frac{(T_i - T_a)}{G_T} \right] \quad (4)$$

The ABNT standard NBR10184 (1988) specifies the procedures for the determination of the instantaneous collector efficiency and suggests that the tests should be performed outdoors, close to real operation conditions. These standards establish the experimental procedures, requirements of accuracy, meteorological conditions, etc. The method can be summarized in the following steps:

- The water at collector inlet is fixed to a certain temperature;
- The inlet, outlet and ambient temperatures, the water flow and the irradiance on the collector plane are registered;
- The efficiency is calculated from the relation between the useful energy and the incident irradiance;
- The tests should be made, if possible, in nearly symmetrical pairs for each inlet temperature, one before and one after the noon;
- At least 16 points are registered.

The efficiencies are plotted as a function of $(T_i - T_a)/G_T$. A linear regression of the points results in the instantaneous efficiency curve.

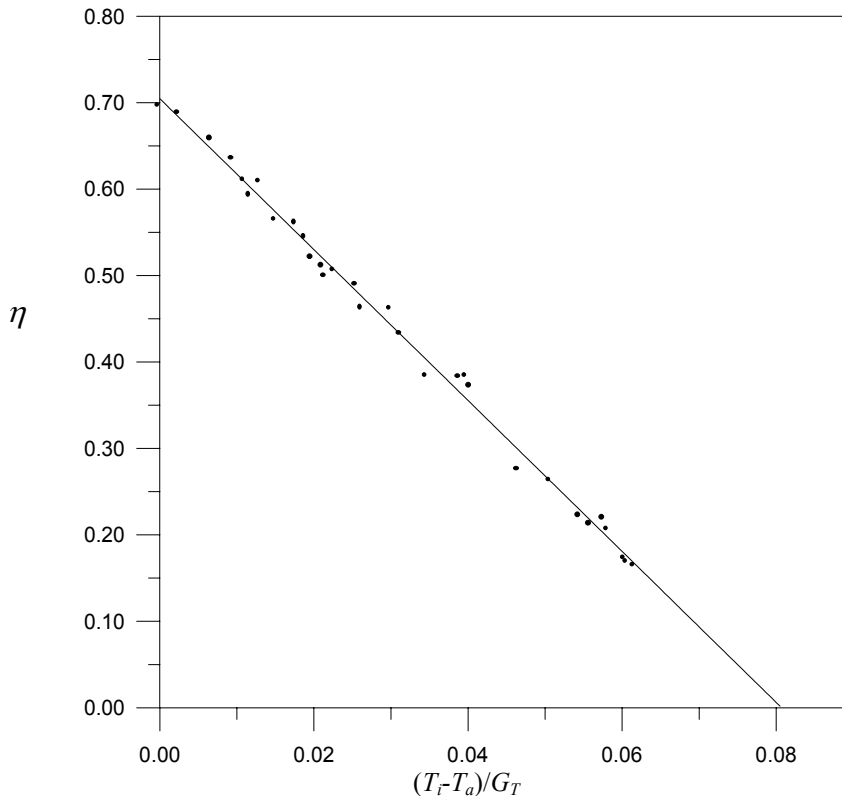


Figure 4. Measured instantaneous efficiency curve of IEM solar collectors.

The Solar Energy Laboratory of UFRGS is provided with a test facility for the experimental determination of the performance of solar collectors. This equipment, called Aquatherm WS88, is capable to maintain the inlet temperature and the water flow within the limits prescribed by the standard. Up to two collectors can be tested simultaneously. This feature can be very useful to detect small performance differences between collectors due to minor constructive modifications, since the water circulates through both collectors in a closed loop, ensuring that the water flow is the same for both collectors. The inlet temperature of each collector can be individually adjusted from 20 °C to almost 100 °C, with a stability of 0.1 °C. The water flowing from the second collector goes to a heat exchanger, dropping its temperature to a few degrees below the desired inlet temperature for the first collector. The water is then heated to the set temperature by bursts of power dissipated by electrical heaters and sent to the first collector inlet. The same goes for the second collector. The water flow, measured by a volumetric flow meter with an electrical output, can be adjusted between 70 and 200 l/h. The irradiance on the collector plane and the wind speed are sensed by an Eppley PSP pyranometer and a cup anemometer. Temperatures are sensed by platinum resistance sensors measured with the 4-wire method.

The collectors are mounted on a metallic cart and positioned in a suitable solar orientation. The tests are performed in days of clear and unclouded sky. The wind speed must be inferior to 2 m/s. The inlet temperatures of each collectors and the water flow rate are set prior to starting the test. To be considered a valid point, the fluctuations of the irradiance, inlet temperature and water flow must be within respectively $\pm 50 \text{ W/m}^2$, 0.3 °C and $\pm 2 \%$ during a period no shorter than the time constant of the tested collector. In this case was adopted a period of 15 min. In practice, the process of collecting the minimum of 16 points can be very time consuming, taking several days.

The collectors were tested according to the described procedures and the resulting curve is shown in Fig. (4). The fitted line intercepts the Y axis at $F_R(\tau\alpha)_e$ and its slope is given by $F_R U_L$.

2.3. Instant gas heaters

The chosen devices to be used as auxiliary energy source were automatic instant gas heaters, manufactured by Komeco (model KO 550S), which satisfied the minimum requirements for this application with a reasonable price. Its maximum flow and efficiency, according to the catalogue, are 7.5 l/min and 81 % respectively. Although this model was specific for LPG, the results are compatible with natural gas heaters.

The ABNT standard NBR8130 (1998) specifies the minimal requirements and procedures for the performance determination of instant gas heaters with gas fuel.

The gas heater efficiency was calculated from the expression:

$$\eta = \frac{m C_p (T_o - T_i)}{V_0 HHV} \quad (5)$$

where m is the heated water mass, T_i is the gas heater inlet temperature, T_o is the gas heater outlet temperature, HHV is gas higher heating value and V_0 is the gas consumption at the HHV standard conditions (273 K, 101.3 kPa, dry).

The correction of the measured gas volume to the higher heating value standard conditions can be performed through Eq.(6):

$$V_0 = V \frac{P_a + P - W}{101.3} \frac{273}{T_g} \quad (6)$$

where V is the measured gas volume in m^3 , P_a is the atmospheric pressure in kPa, P is the pressure of the gas in kPa, W is the partial vapor pressure in kPa and T_g is the gas temperature in K near the gas meter.

The experiment was assembled and conducted according to the referred standard. It was found an average efficiency of 81 % for the employed heater, which agreed to the catalogue value. Tests using inlet temperatures beyond those established by the standard were also performed showing no significant variation in the efficiency.

The amount of power delivered to the water by the gas heater can be adjusted between 8000 and 13000 W through the gas flow control valve.

3. Data acquisition system

The temperatures at the inlet and outlet of the solar collectors, at the connections of the collector to the tank and at the connections of the gas heater to the tank are measured with platinum resistance sensors (Pt100). The tank internal temperatures, cold and consumption water and ambient air temperatures are measured with integrated circuit sensors (LM35). The placement of the temperature sensors is the same for both systems.

A Pt100 is a device constituted by a platinum wire or film which electrical resistance is 100 Ω at 0 °C and varies with the temperature according to the equation:

$$R = R_0 (1 + \alpha T) \quad (7)$$

where R is the sensor measured resistance, R_0 is the sensor resistance at $0\text{ }^\circ\text{C}$, α is the platinum temperature coefficient and T is the sensor temperature in $^\circ\text{C}$.

All of the employed Pt100 sensors were calibrated simultaneously with the help of a Lauda thermostatic bath device. The sensors were immersed in stirring water with temperatures varying from 15 to $60\text{ }^\circ\text{C}$ in steps of $5\text{ }^\circ\text{C}$. The sensors were connected to the data acquisition system employing the 4-wire configuration. Linear regressions of the obtained points resulted in a straight line calibration equation for each sensor.

The LM35 is an integrated circuit that outputs a DC voltage proportional to its temperature ($10\text{ mV}/^\circ\text{C}$). The choice in favor of this sensor to measure the temperature of the water inside the tank, besides lower cost and more sturdiness when compared to the fragile Pt100, was due to the lower number of required wires. Since these devices have only three terminals (Vcc, GND and Output), for n temperature sensors are required $n + 2$ wires (against $n \times 4$ in the case of the Pt100). Thus, the lower number of copper wires inside the tank translates in lower thermal conductance in the axial direction, which could mask the readings of the sensors. Eight LM35, corresponding to each tank layer, were installed equally spaced along the tank wet height. They were assembled inside a 15 mm diameter CPVC tube to ensure that water or wetness would not provoke voltage leakage between sensors terminals, as occurred while testing other possible mechanical solutions. The higher thermal capacity and longer time response were minimized by soldering a small copper fin to one of the terminals of each sensor. This terminal was bent in such a way to press the fin against the internal tube wall. A low-pass filter was added to the output of each LM35 in order to minimize the high frequency noise. The “sensor tube” was calibrated inside a second (50 mm diameter) tube attached to the external loop of the thermostatic bath. Thus, during the calibration process, the bath water flowed in the gap between the tubes, ensuring that all the length of the sensor tube was at a homogenous temperature.

The irradiance on the solar collector plane was measured with a photovoltaic pyranometer (Zanenco, 1991) calibrated to an Eppley PSP pyranometer.

The gas consumption is registered by volumetric totalizers manufactured by Laos. The readings of these meters are used to check the gas consumption estimated by the data acquisition program from the time while the gas burners were activated.

All the sensors signals are registered by a HP34970A data acquisition unit interfaced to a computer via RS-232. A computer program developed in Quick Basic coordinates the data acquisition and commands the solenoid valves that control the consumption of water. The scan rate is 40 seconds.

4. Experimental results

The water inside both tanks was heated to the same temperature and homogenized prior the data acquisition program was launched. Figure (5) presents the profile of the mean temperatures inside each tank, as well as their thermal losses and the ambient temperature. It can be observed that the mean temperatures inside both tanks were the same until the dawn of the first day, when the thermostats activated the gas heaters of both systems. Then, due to the differences between configurations, the *parallel* system reaches the higher temperatures, resulting also in higher losses.

The solar collectors deliver energy to the tank during the daytime, provoking a smooth and continuous rising of the temperature of both systems. Since the ambient temperature is usually higher, the thermal losses are decreased during these periods. The reverse occurs at nighttime, when ambient temperature drops, resulting in an increase of the thermal losses. One can observe that at daytime periods the mean temperature of the *series* system tank is higher than in the *parallel* system tank, indicating a higher solar energy gain under *series* configuration.

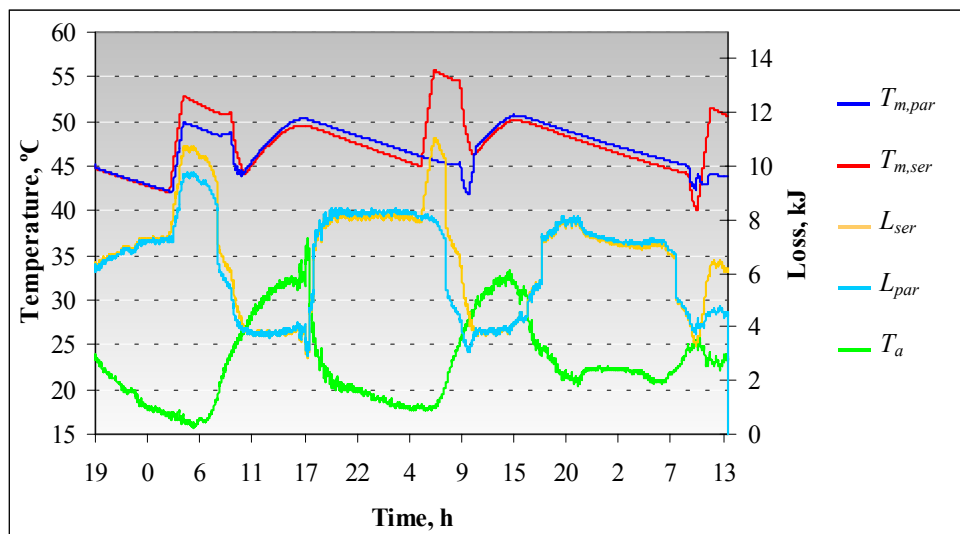


Figure 5. Mean temperatures of the water inside the tanks, ambient temperature and tanks thermal losses along a period of three days.

The set point and positioning of the thermostats that control the gas heaters are the same for both systems, respectively 46 °C and 66 cm from the bottom (corresponding to layer 5). Figures (6) and (7) represent one of the periods in which the gas heaters were operating and the effects on the temperature profile inside the tanks of each configuration. In Figure (6) can be observed an even temperature rise, with constant temperature differences between tank layers of the *parallel* system, while Fig. (7) shows that only layers 7 and 8 of the *series* system had their temperatures significantly increased. In this case the temperature stratification was enhanced, with a more pronounced difference in temperature between superior and inferior layers.

For both systems the inlet water of the solar collectors comes from the tank bottom, where temperatures are lower. One can observe in Fig. (8) the temperature rise of the solar collectors of each system. So if the inlet temperature of the collectors of the *series* system is lower and the remaining variables of Eq. (4) are approximately the same for both systems, it is confirmed the superior thermal gain from the solar collectors on the *serial* system.

In Figure (9) are represented the temperature profiles of the tanks along the same period of Fig. (7), showing the stronger temperature stratification inside the *series* system tank. This temperature distribution is desirable as the load is supplied with hotter water and the colder water from the bottom of the tank goes to the inlet of the solar collectors.

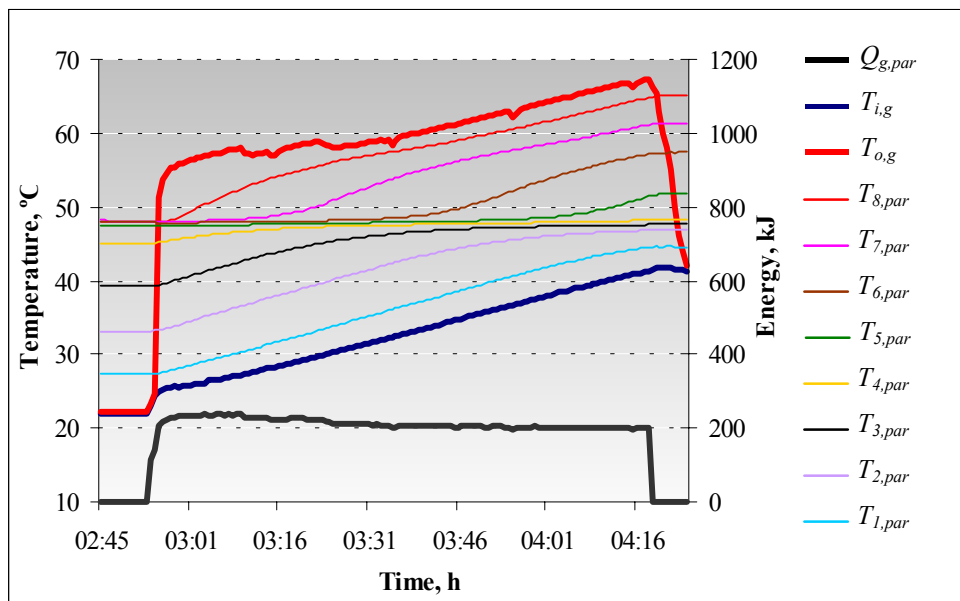


Figure 6. Development of the temperature profile inside the *parallel* system tank when the gas heater is activated. T_1 to T_8 are the temperatures inside the tank. $T_{i,g}$ and $T_{o,g}$ are the water temperature at the inlet and outlet of the gas heater. Q_g is the energy gain transferred from the gas heater to the water.

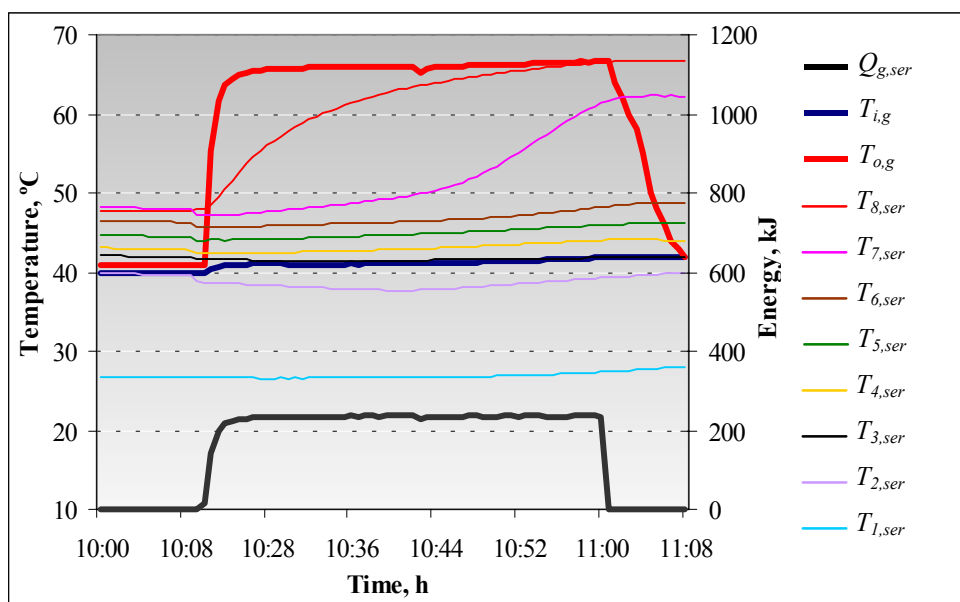


Figure 7. Development of the temperature profile inside the *series* system tank when the gas heater is activated.

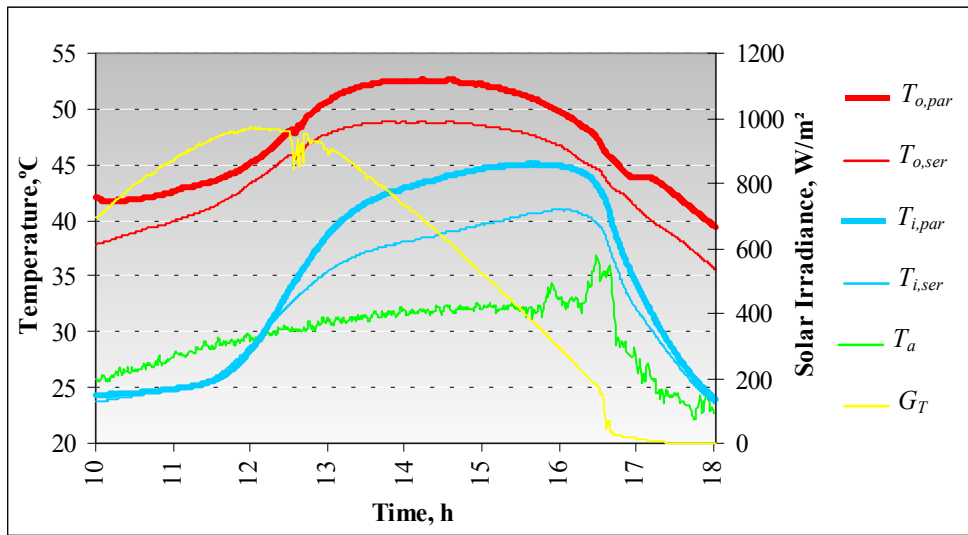


Figure 8. Temperatures of the water at the inlet and outlet of the solar collectors of each system.

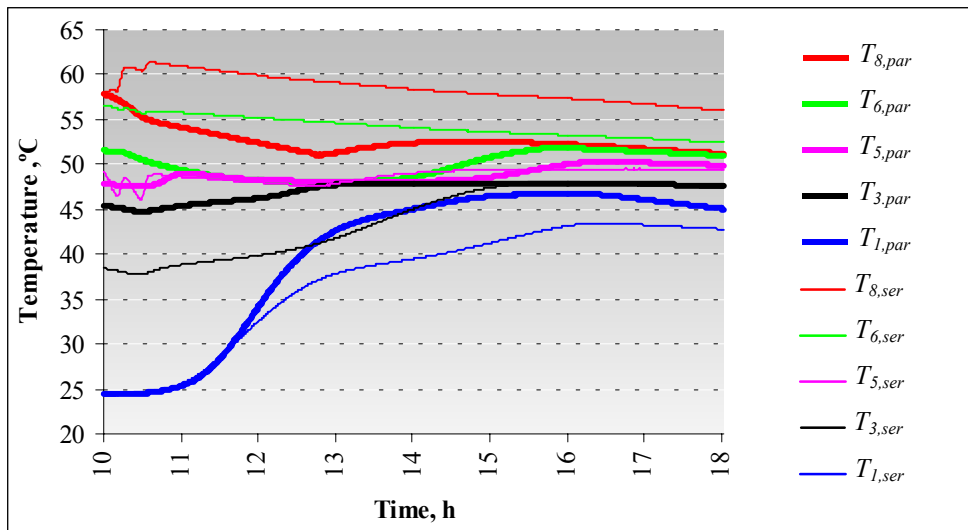


Figure 9. Temperatures of correspondent layers of the tanks of both systems.

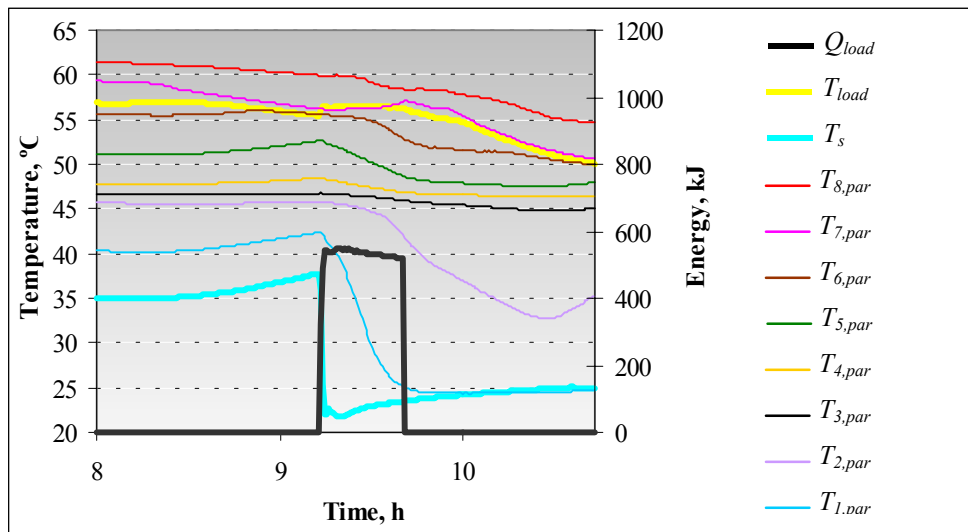


Figure 10. Effects of the load on the layer temperatures of the *parallel* system tank. Q_{load} is the energy associated to the hot water consumed at the T_{load} temperature. T_s is the temperature of the cold water supply.

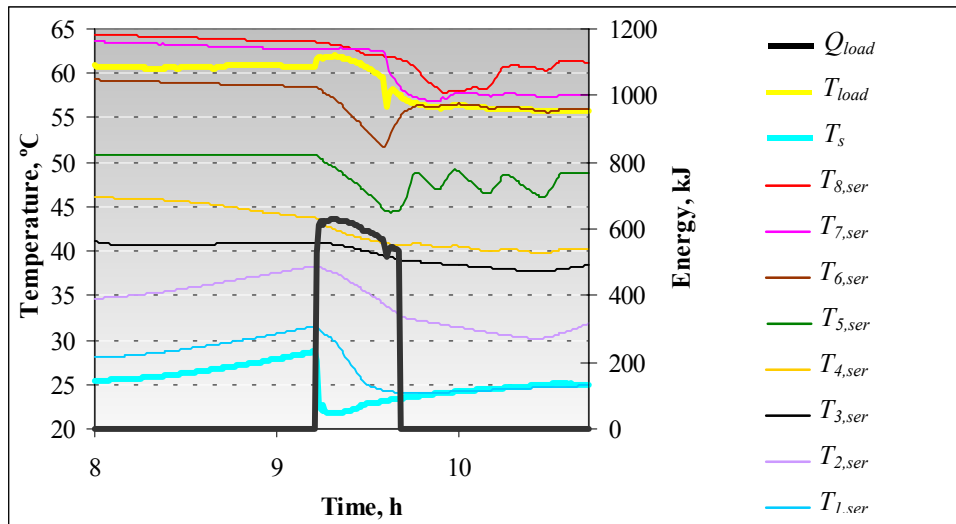


Figure 11. Effects of the load on the layer temperatures of the *series* system tank.

Figures (10) and (11) show the impact of the hot water demand on the temperature profile inside the tanks. The hot water consumption starts always at 9h20min and lasts 30 min in both systems. It can be observed in Fig. (10) that the demand temperature of the *parallel* system remained constant over the period of consumption. The same was not true for the *series* system, as shown in Fig. (11), due to the differences of the temperature gradients in the upper layers of each system.

Table 1 presents a comparison between the results of both systems concerning the efficiency of the solar collectors, the tank thermal loss, the energy associated to the gas consumption, the variation of the stored energy and the energy associated to the load after three days. The variation of the stored energy was calculated taking into account the difference between the initial and final mean temperatures of the tank and it was negative in the case of the *series* system because the final mean temperature was lower than the initial. The energy delivered by the gas heater was significantly higher in the *parallel* system than in the serial system. The load energy of the *parallel* system was also higher but not at the same rate of the gas consumption. The lower overall losses of the *parallel* system indicated that more energy was wasted in this configuration for the tested load profile.

Table 1. Energy balance of both systems.

	Parallel system	Series System
Solar collector efficiency (%)	56	60
Solar energy gain (MJ)	45.9	48.5
Tank energy variation (MJ)	14.2	-3.4
Hot water load (MJ)	68.8	60.5
Gas energy gain (MJ)	95.0	56.2
System thermal losses (MJ)	57.9	40.8

5. Conclusions

The system components were successfully characterized, transferring reliability to the obtained results. The gas heaters were tested following the conditions prescribed by the standards and efficiency tests with higher temperatures were also performed. The curve of instantaneous efficiency of the solar collectors was experimentally determined, as well as the tanks thermal loss coefficient. The data acquisition system was shown to be suitable and dependable.

Experimental results were obtained from the monitoring of the systems assembled with the two proposed configurations. Although these preliminary results are limited to the tested load profiles, they are pointing to the *serial* system as the more efficient configuration. This work will be continued in the next months, including experimental tests with different configurations and load profiles. These data will permit a deeper understanding of the phenomena associated to such systems and to establish a broader sizing methodology.

A computer program for the simulation of the behavior of temperatures of the proposed configurations was validated with data originated from this experiment. This program is the subject of another work to be presented at this congress.

6. Acknowledgement

This work is part of a project sponsored by FINEP and PETROBRAS. Authors are supported by Conselho de Desenvolvimento Científico e Tecnológico – CNPq.

7. References

- Associação Brasileira de Normas Técnicas, 1988. “Coletores Solares Planos para Líquidos - Determinação do Rendimento Térmico (NBR10184)”, Rio de Janeiro, Brazil.
- Associação Brasileira de Normas Técnicas, 1998. “Aquecedor de Água a Gás Tipo Instantâneo – Requisitos e Métodos de Ensaio (NBR8130)”, Rio de Janeiro, Brazil.
- Duffie, J.A., Beckman, W.A., 1991. “Solar Engineering of Thermal Processes”, John Wiley & Sons Inc. New York, USA, pp. 250-286.
- Krenzinger, A., Lafay, J.M., 2002. “Análise Experimental de Um Sistema de Aquecimento de Água Com Energia Solar e Gás”, Proceedings of the 9th Congress of Thermal Engineering and Sciences, Caxambu, Brazil.
- PROCEL, 2003. Programa Nacional de Conservação de Energia Elétrica, www.eletrobras.gov.br/procel/.
- Zanescio, I., 1991. “Análise e Construção de Um Piranômetro Fotovoltaico”, PROMEC, Universidade Federal do Rio Grande do Sul, Porto Alegre, Brazil.